Stiffness of desiccating insect wings

COMMUNICATION

Stiffness of desiccating insect wings

T E Mengesha[1], R R Vallance[1] and R Mittal[2]

[1] Department of Mechanical Engineering, The George Washington University, 738 Phillips Hall,
801 22nd St NW, Washington, DC 20052, USA
[2] Department of Mechanical Engineering, Johns Hopkins University, 126 Latrobe Hall,
3400 N Charles Street, Baltimore, MD 21218, USA

E-mail: vallance@gwu.edu

Abstract
The stiffness of insect wings is typically determined through experimental measurements.
Such experiments are performed on wings removed from insects. However, the wings are
subject to desiccation which typically leads to an increase in their stiffness. Although this
effect of desiccation is well known, a comprehensive study of the rate of change in stiffness of
desiccating insect wings would be a significant aid in planning experiments as well as
interpreting data from such experiments. This communication presents a comprehensive
experimental analysis of the change in mass and stiffness of gradually desiccating forewings of
Painted Lady butterflies (*Vanessa cardui*). Mass and stiffness of the forewings of five
butterflies were simultaneously measured every 10 min over a 24 h period. The averaged
results show that wing mass declined exponentially by 21.1% over this time period with a time
constant of 9.8 h, while wing stiffness increased linearly by 46.2% at a rate of 23.4 μN mm^{-1}
h^{-1}. For the forewings of a single butterfly, the experiment was performed over a period of
1 week, and the results show that wing mass declined exponentially by 52.2% with a time
constant of 30.2 h until it reached a steady-state level of 2.00 mg, while wing stiffness
increased exponentially by 90.7% until it reached a steady-state level of 1.70 mN mm^{-1}.

1. Introduction

Insects achieve flight by generating aerodynamic forces through a combined effect of a flapping motion and the dynamic deformation of their wings. The flexibility of the wings is an important factor that influences flight performance through fluid–structure interaction with the surrounding air [1–3]. The flexibility of insect wings is maintained through cuticular hydration induced by circulating hemolymph [4, 5]. Insects prevent desiccation by raising the level of water content in their body, by remaining inactive to minimize loss of water, or by developing an increased tolerance to loss of water [6–8].

The structural stiffness of insect wings is typically determined through experimental measurements conducted on the wings of freshly sacrificed insects [9, 10]. Desiccation can cause significant increase in the structural stiffness of wing samples, leading to a deterioration of their natural compliance [11, 12]. Researchers usually minimize the effects

of desiccation by either conducting the experiment quickly or by raising the ambient humidity level, for example by placing wing specimens in a humidity chamber or by placing wet tissue near the wing specimen [9, 13].

This communication provides insights into the gradual changes of mass and stiffness of insect wings during desiccation. Mass and stiffness were measured simultaneously every 10 min, over a 24 h period for the forewings of five Painted Lady butterflies, and over a 1 week period for the forewings of a single Painted Lady butterfly. The results show that desiccation caused significant changes in both mass and stiffness of the wings. For example, mass declined by 21.1% and stiffness increased by 46.2% within 24 h after sacrificing the butterflies.

Erroneous measurements of mass and stiffness can have considerable consequences on computational studies of insect flight. The mechanics of insect flight is often used as the basis for the design of flapping micro-aerial vehicles (MAVs).
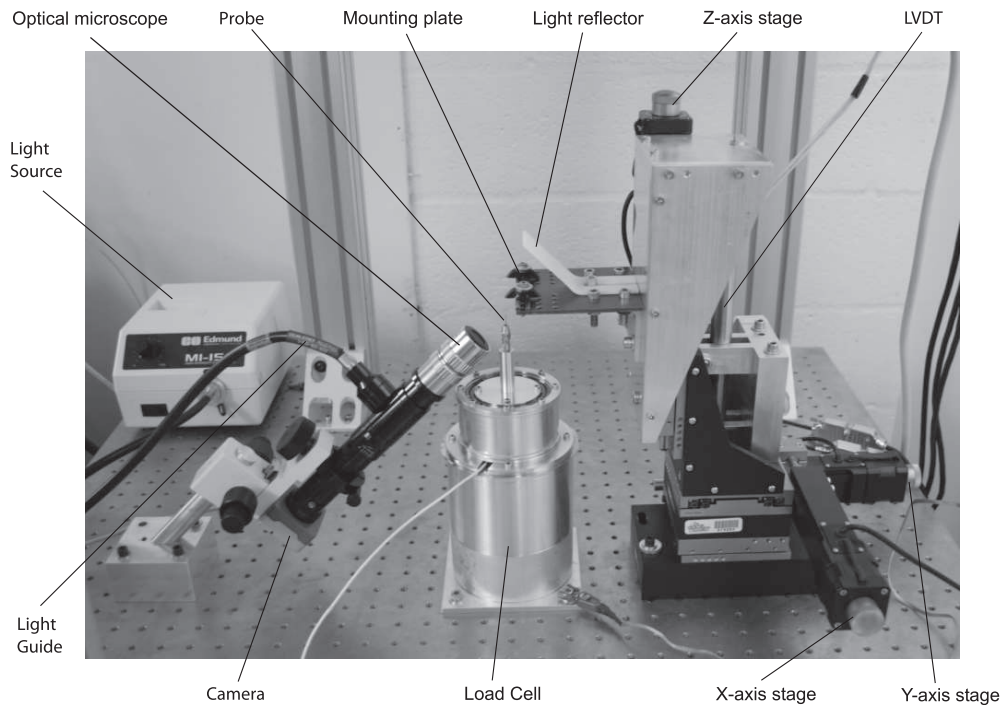
Figure 1. Experiment apparatus for measuring wing stiffness during desiccation.

Incorrect analyses of insect flight can consequently lead to flawed designs of MAVs. Therefore, the effects of desiccation on the structural attributes of inertia and stiffness must be fully recognized, and preventive measures must be taken to minimize the changes on the properties of wing specimens during experimental measurements. The results presented in this communication show that the influence of desiccation can be effectively reduced by using fresh specimens in limited duration of experiments. For example, the changes in mass and stiffness of the butterfly wings in the first hour of measurement were only 2.5% and 1.8%, respectively.

2. Materials and methods

The mass of the butterfly forewings was measured on a Sartorius™ CPA225D analytical balance. The dual-range analytical balance had a fine resolution of 0.01 mg with a measuring capacity of 0–100 g and a coarser resolution of 0.1 mg with a range of 100–220 g. The balance was operated through Labview software from a desktop computer.

During the experiment, automated manipulation of the butterfly wing was enabled by a linear motion system with three degrees of freedom (Thorlabs™, model LNR50S). The stage was equipped with three stepper motors, operated through a controller that was connected to a desktop computer and programmed in Labview software. The travel range of the stage was 0–50 mm in each axis. The vertical displacement of the three-axis stage was measured by a Sentech™ 75DC-1000 linear variable differential transformer (LVDT) to provide a convenient analog measurement.

A custom-designed load cell was placed next to the three-axis stage as shown in figure 1. The load cell had a resolution

of 19 μN with a range of 0–76 mN, and it was specifically designed to measure only vertical forces. A probe, made of a stainless-steel rod with a diameter of 0.025 in and a rounded tip, was vertically affixed on top of the load cell. The purpose of the probe was to push the butterfly forewing at a selected measurement point and transfer the vertical force that was generated by the bending forewing to the load cell. The tip of the probe was monitored through a camera (Motic™, model Moticam 2000) attached to an optical microscope as shown in figure 1. The live view from the optical microscope provided visual confirmation while positioning the butterfly forewing above the probe's tip.

One forewing was cut off at the thorax of a live butterfly, and it was immediately placed on the analytical balance. The butterfly was then mounted on a steel plate with its second forewing outstretched and clamped at the thorax as shown in figure 2(a). The steel plate was fastened on the three-axis stage as shown in figure 1. As shown in figure 2(b), a measurement point was selected at the middle of the cubital vein (Cu_1) of the butterfly forewing. Next, the probe tip was aligned with the measurement point on the butterfly forewing by adjusting the coordinates of the three-axis stage from the desktop computer. The live view from the optical microscope was used to navigate the wing and place the probe tip as close as possible without direct contact. Once proper alignment was confirmed, the coordinates of the three-axis stage were recorded, and the measurement process was initiated.

The measurement process was fully automated and coordinated through a single Labview program. Both mass and stiffness were measured synchronously. The load cell and LVDT were initiated at the start of the measurements. Then, the z-axis stage was moved vertically downward by 0.5 mm,
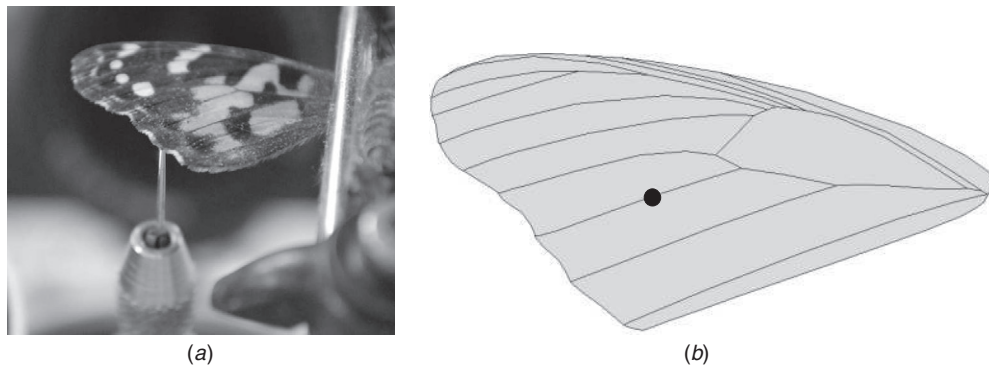
Figure 2. (*a*) The outstretched forewing of a Painted Lady butterfly positioned above the probe during the experiment, and (*b*) the measurement point (shown as a dark circle) located at the middle of the cubital vein (Cu_1) of the wing.

and the position was held for a 10 s dwell. While the stage was in its dwell position, the analytical balance measured the mass of the butterfly forewing. Then, the stage moved down another 0.5 mm, and the mass was measured again while the stage dwelled another 10 s. The stage lowered a total of 1 mm in the downward direction. The downward travel led to contact between the wing and the tip of the probe, and the contact force caused the wing to bend upward. The bent wing pushed downward on the tip of the probe, generating the vertical force that was measured by the load cell.

Next, the stage was slowly moved upward by 0.5 mm, and after a 10 s dwell it was moved upward again by 0.5 mm; mass was measured during each dwell. The upward travel gradually decreased the vertical force, and the wing eventually disengaged from the tip of the probe. During the downward and upward travel of the stage, the vertical force and displacement were continuously measured by the load cell and LVDT, respectively. The data acquired from the load cell, LVDT, and analytical balance were saved in text files. These text files were post-processed to evaluate the mass and stiffness of the butterfly forewings. This completed the first measurement of mass and stiffness, and a 10 min interval was initiated.

The butterfly was sacrificed immediately after the completion of the first measurement. This was done carefully, to avoid corrupting the measurement process by inadvertently touching the butterfly's forewing. After a 10 min interval, a second cycle of measuring force, displacement and mass was initiated for the forewing of the now dead butterfly. The measurement was repeated every 10 min over the duration of the experiment, which was 24 h for five Painted Lady butterflies, and 1 week for a single butterfly. A total of 116 and 812 measurement cycles were performed for the periods of 24 h and 1 week, respectively.

During the experiments, room temperature and relative humidity were measured simultaneously every 15 s by a programmable meter (Omega^{TM}, model HH314A). The meter was connected to a desktop computer, and it was programmed through a stand-alone software. The measurement range of the meter was 0–100% with a resolution of 0.1% for relative humidity, and −4–140°F with a resolution of 0.1°F for temperature.
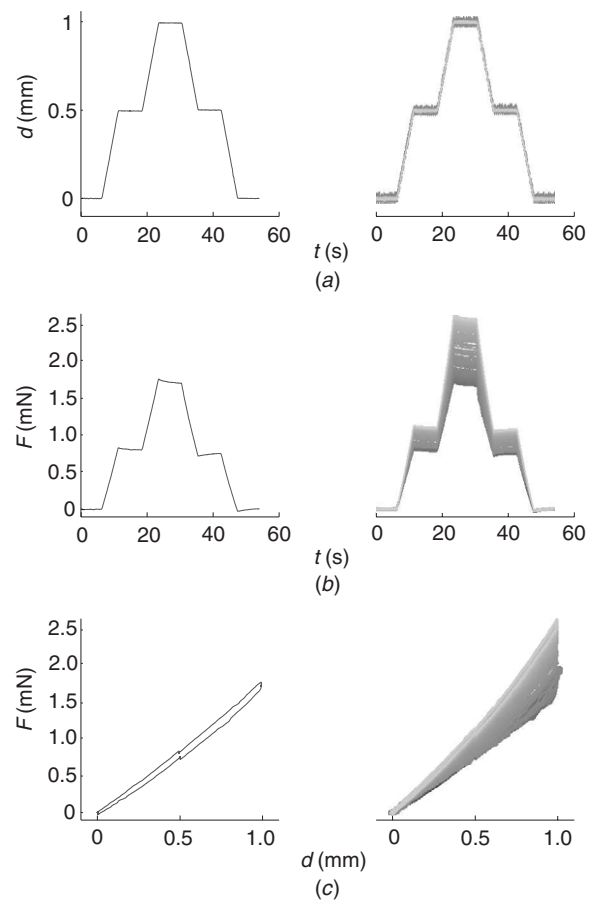
Figure 3. Plots of the data measured by the load cell and LVDT over 24 h for a butterfly forewing: (*a*) displacement versus time, (*b*) force versus time and (*c*) force versus displacement.

3. Results

Figure 3 shows data acquired from the load cell and LVDT during the stiffness measurement of the forewing of a Painted Lady butterfly over 24 h. The first plot in figure 3(*a*) shows the wing displacement as a function of time during the first measurement cycle. The wing displacement was the vertical deflection of the measurement point relative to the clamped edge of the wing. The displacement–time curves of all 116
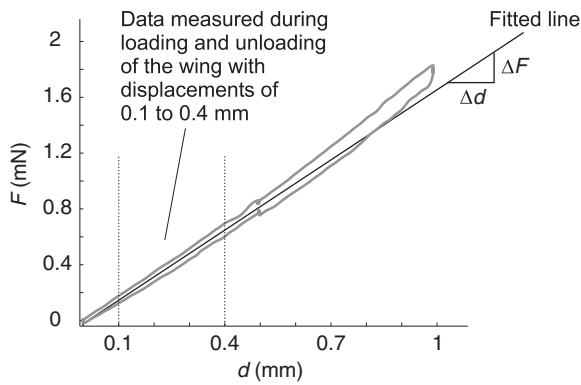
Figure 4. Determining stiffness from the slope of a line fitted through the data measured during loading and unloading of the wing with displacements of 0.1–0.4 mm.

measurement cycles are superimposed in the second plot of figure 3(*a*) by setting the starting time of each measurement cycle to zero. The displacement–time curves are overlapping, since the downward and upward travel of the three-axis stage was nearly identical for all measurements. Figure 3(*b*) shows the force–time plot for the first measurement cycle, followed by a plot with the superimposed force–time curves of all 116 measurement cycles. The superimposed curves were

plotted with fading shades of gray, where the darkest curve corresponds to the first measurement cycle.

The first plot in figure 3(*c*) shows the measured force as a function of the wing displacement during the first measurement cycle. The second plot in figure 3(*c*) shows the force–displacement curves of all cycles superimposed with fading shades of gray. The slope of each force–displacement curve equals the static stiffness of the wing at the measurement point. The rising slope in the force–displacement curves clearly shows that the wing stiffened as a consequence of its gradual desiccation over 24 h. A curve-fitting technique was used to determine the stiffness *k* of each measurement cycle. As shown in figure 4, a line was fitted through the data measured during loading and unloading of the wing with displacements of 0.1–0.4 mm. The slope of the fitted line was then evaluated using equation (1), where *F* and *d* are the measured bending force and wing displacement, respectively,

$$ k = \frac{\Delta F}{\Delta d}. \tag{1} $$

Mass and stiffness were measured for the forewings of five Painted Lady butterflies over 24 h. Figure 5 shows plots of the measured mass, stiffness, room temperature and relative humidity as functions of the measurement time. The plots show that the wing mass decayed exponentially, while the stiffness of the wings increased linearly.
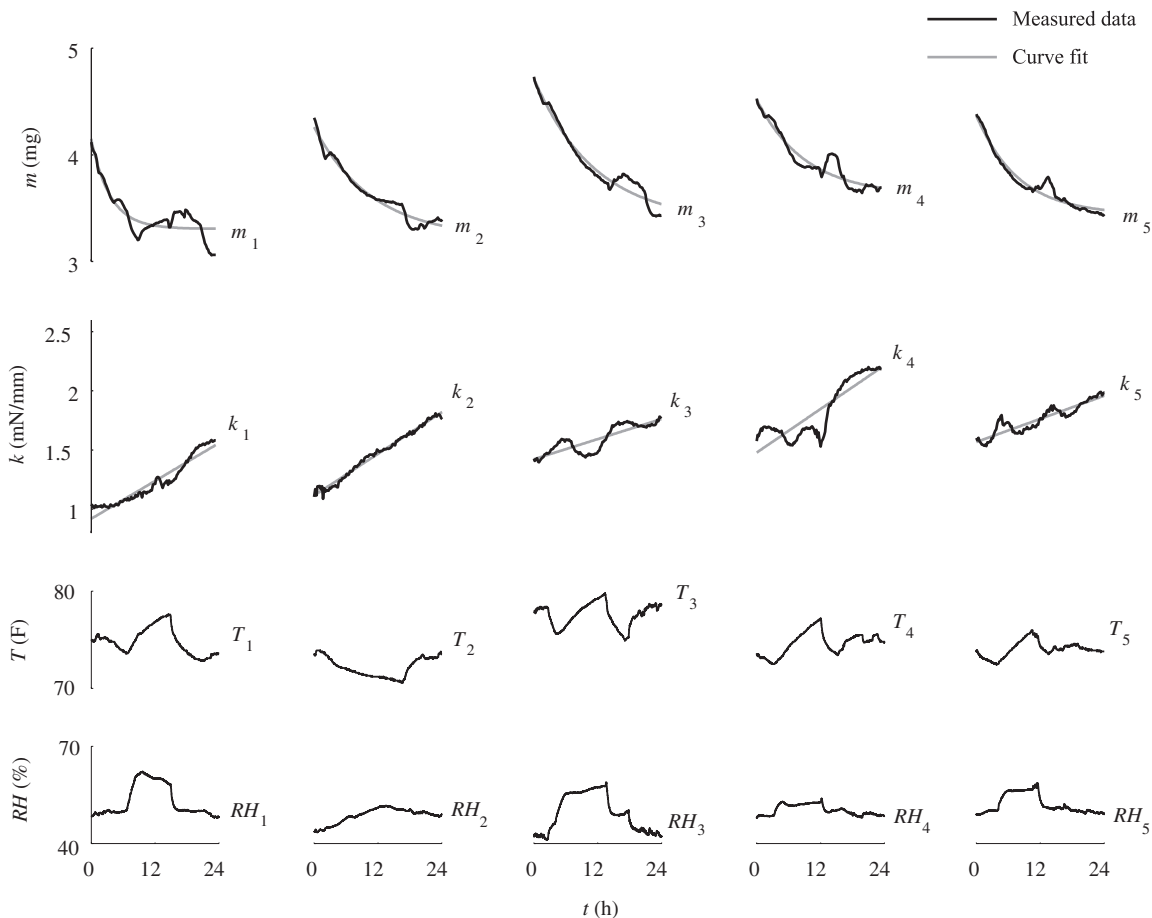
Figure 5. Mass (*m*), stiffness (*k*), room temperature (*T*) and relative humidity (*RH*) measured over 24 h for the forewings of five Painted Lady butterflies.

Table 1. Mass measurement for the forewings of five Painted Lady butterflies over 24 h.

Butterfly	m_o (mg)	m_f (mg)	τ (h)
1	4.15	3.31	3.58
2	4.26	3.22	11.09
3	4.72	3.37	11.53
4	4.52	3.62	9.09
5	4.37	3.44	7.94

Table 2. Stiffness measurement for the forewings of five Painted Lady butterflies over 24 h.

Butterfly	k_o(mN mm^{-1})	β(mN mm^{-1} h^{-1})
1	9.19e−1	2.67e−2
2	1.12e0	2.93e−2
3	1.42e0	1.42e−2
4	1.48e0	3.07e−2
5	1.57e0	1.63e−2

The exponential decay of the wing mass was modeled as shown in equation (2), where m_o and m_f are the initial and final mass values, respectively, and τ is the time constant. The values of m_o, m_f and τ were determined by a least-squares algorithm, which used equation (2) to find the best-fit exponential decay for the measured mass. Table 1 lists the values of m_o, m_f and τ for the forewings of the five Painted Lady butterflies:

$$m(t) = m_f + (m_o - m_f) \, \mathrm{e}^{(\frac{-t}{\tau})}. \tag{2}$$

The wing stiffness was modeled as a function of time as shown in equation (3), where k_o is the initial stiffness value and β is the rate of change in stiffness. The values of k_o and β were evaluated by a least-squares algorithm, which determined the best-fit line to the measured stiffness values. Table 2 lists the values of k_o and β for the forewings of the five Painted Lady butterflies:

$$k(t) = k_o + \beta t. \tag{3}$$

Mass and stiffness were measured over a 1 week period for the forewings of a single Painted Lady butterfly, in order to investigate the long-term effects of desiccation. A total of 812 measurement cycles were performed during the 1 week period. Figure 6 shows the measured mass, stiffness, room temperature and relative humidity as functions of the measurement time. The wing mass decayed exponentially until it reached a steady-state level. The exponential decay was modeled with equation (2), and a least-squares algorithm was used to find the best-fit exponential curve to the measured mass. The corresponding equation is shown in figure 6, where the values of m_o, m_f and τ are 4.20 mg, 2.00 mg and 30.2 h, respectively.

The increase in wing stiffness was modeled using the modified logistic function shown in equation (4) [14, 15], where k_o and k_f are the initial and final stiffness values, respectively. The parameters q and t_q are the maximum growth rate and the corresponding time. The values of k_o, k_f, q and t_q were evaluated by a least-squares algorithm, which used equation (4) to determine the best-fit curve for the
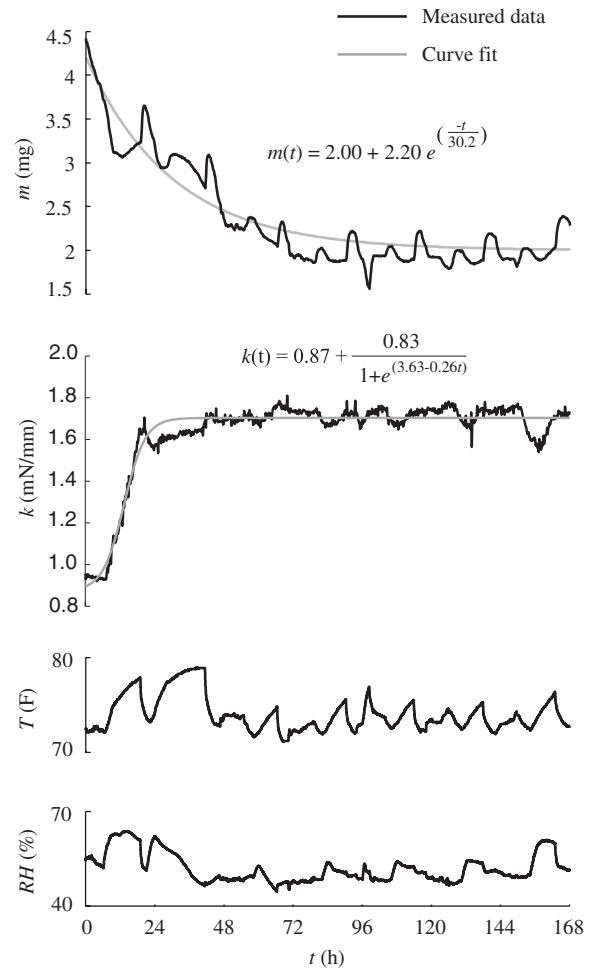
Figure 6. Mass, stiffness, room temperature and relative humidity measured over a 1 week period for the forewings of a single Painted Lady butterfly.

measured stiffness data. The corresponding stiffness equation is shown in figure 6, where the values of k_o, k_f, q and t_q are 0.87 mN mm^{-1}, 1.70 mN mm^{-1}, 0.26 h^{-1} and 13.6 h, respectively:

$$k(t) = k_o + \frac{k_f - k_o}{1 + \mathrm{e}^{[-q(t-t_q)]}}. \tag{4}$$

4. Discussion

The aforementioned experiments were not conducted in a temperature and humidity controlled room; hence, some fluctuation is evident in both room temperature and relative humidity as shown in figures 5 and 6. Fluctuations are also apparent in the measured mass and stiffness data as shown in figures 5 and 6. Although fluctuation was anticipated as a result of measurement noise from the load cell and electronic balance, figure 6 also shows unexpected increases in the measured mass of the wing. Butterfly wings are hydrophobic by nature [16–18]; hence, water absorption is an unlikely source of such changes.

Two additional experiments were performed to determine whether the aforementioned fluctuations occurred due to some
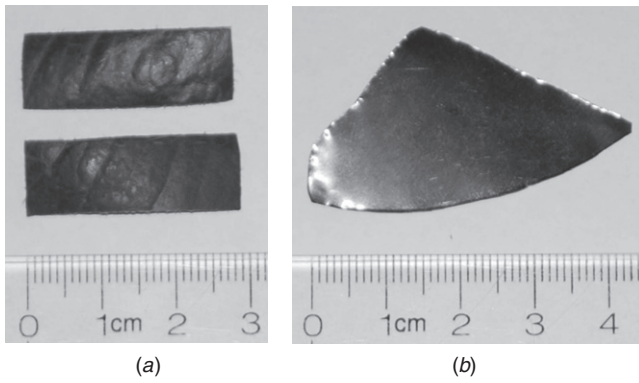
Figure 7. Mass and stiffness were measured for the following objects to determine the sources of measurement fluctuations: (*a*) small strips cut out of an American Holley leaf (*Illex opaca*), and (*b*) a wing-shaped stainless-steel specimen.

specific characteristics of the butterfly wings or simply due to measurement errors. Mass and stiffness were measured over a 24 h period for the following test specimens: (1) small strips cut out of an American Holley leaf (*Illex opaca*) as shown in figure 7(*a*); and (2) wing-shaped pieces cut from a sheet of stainless steel as shown in figure 7(*b*).

The mass of the leaf specimen declined exponentially as shown in figure 8(*a*). Although there is some fluctuation in the mass–time curve, it is obscured by the relatively large range of the measured data. The leaf specimen curled significantly due to desiccation; hence, it was not an appropriate test specimen for the contact-based stiffness measurement process. Figure 8(*b*) shows fluctuations in the measured mass of the stainless-steel specimen. For example, mass increased by 0.25 mg in 2 h (between the 16th and 18th hours of the measurement time). Water absorption is ruled out as the cause of such an increase in mass, since the test specimen is made of stainless steel. This suggests that the fluctuations in mass of the stainless-steel specimen, as well as in the butterfly wings, were most likely caused by measurement errors from the electronic balance. Such errors can occur due to alterations in air buoyancy, as a result of the changes in room temperature, relative humidity and air pressure [19]. Fluctuation is also evident in the measured stiffness of the stainless-steel specimen as shown in figure 8(*b*). This fluctuation is a result of measurement noise from the load cell.

We averaged the data from the experimental measurements of mass and stiffness for the five butterfly forewings. The results show significant changes in both mass and stiffness within 24 h after sacrificing the butterflies.
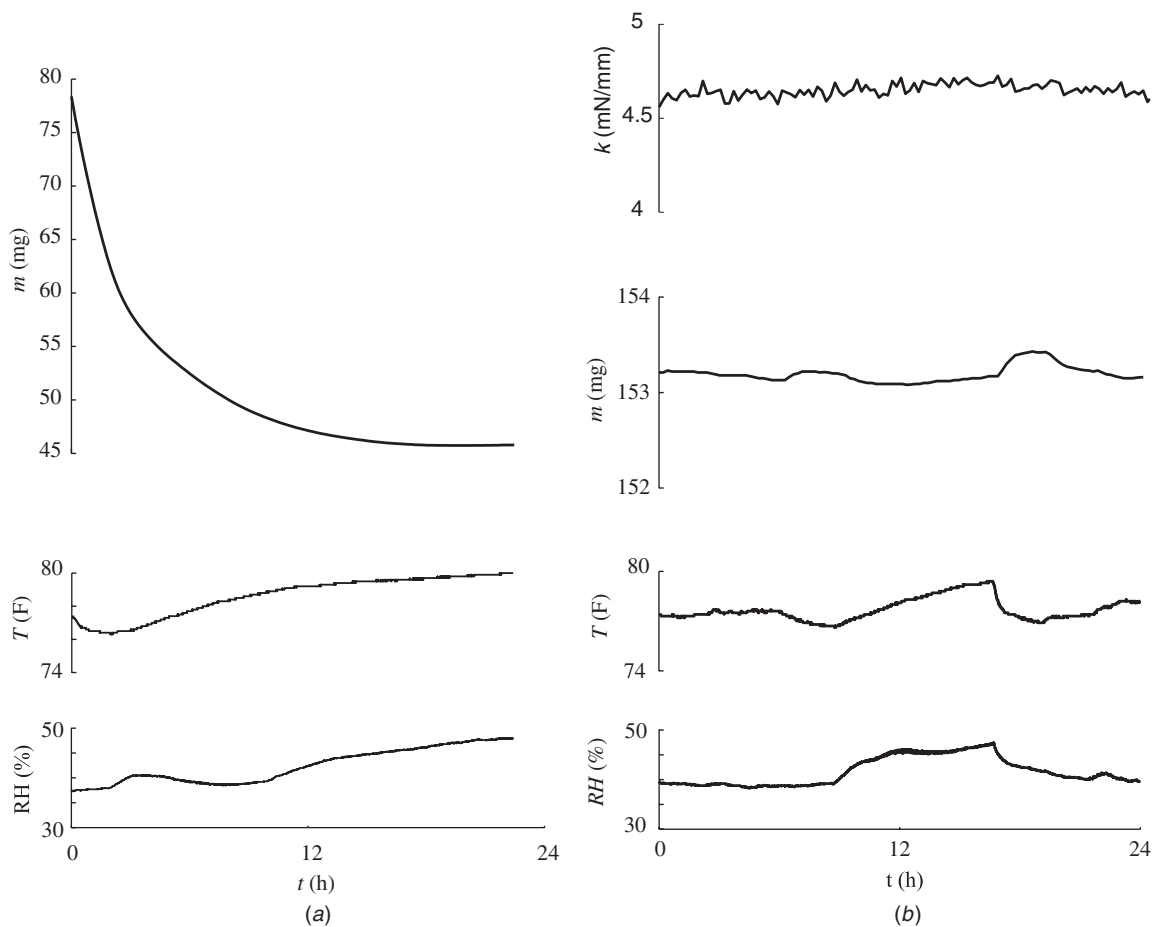
Figure 8. (*a*) Mass, room temperature, and relative humidity measured for a small strip cut out of an American Holley leaf (*Illex opaca*) as shown in figure 7(*a*); and (*b*) mass, stiffness, room temperature and relative humidity measured for wing-shaped specimens cut from a sheet of stainless steel as shown in figure 7(*b*).
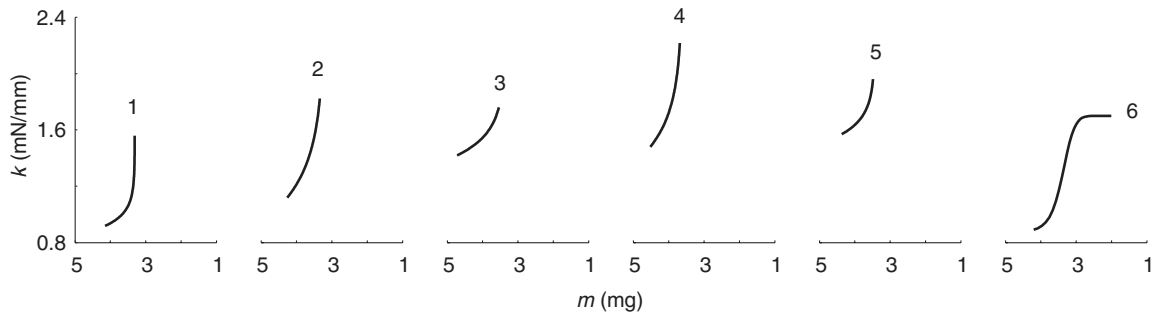
Figure 9. Plots of stiffness as a function of mass of the butterfly wings evaluated using equations (2)–(4). The first five plots correspond to the data measured over 24 h periods, and sixth plot relates to the data measured over a 1 week period.

Wing mass declined exponentially by 21.1% in this period with a time constant of 9.8 h, while wing stiffness increased linearly by 46.2% at a rate of 23.4 μN mm^{-1} h^{-1}. However, only minimal changes occurred in the first hour of the experiments with wing mass and stiffness declining by 2.8% and 1.9%, respectively. This is an important observation that suggests that using freshly sacrificed insects for experimental measurement of the mechanical properties of their wings is a reasonable approach.

The longer duration study, performed over a 1 week period for the forewings of a single butterfly, shows that wing mass declined exponentially by 52.2% with a time constant of 30.2 h until it reached a steady-state level of 2.00 mg, and wing stiffness increased exponentially by 90.7% until it reached a steady-state level of 1.70 mN mm^{-1}.

Figure 9 shows plots of stiffness as a function of mass evaluated using equations (2)–(4). The first five plots correspond to the data measured over 24 h periods for the forewings of five butterflies, and the last plot relates to data from the measurement performed over a 1 week period for the forewings of a single butterfly. The changes in mass and stiffness were evaluated using equations (5) and (6), and were plotted as shown in figure 10. The dark-dashed curve corresponds to Δm and Δk averaged for the five butterflies measured over 24 h periods. The gray vertical lines show the range in Δk for the five butterflies. The dark-solid curve shows Δm and Δk evaluated for the single butterfly measured over a 1 week time. The plot shows a close agreement between the data sets measured over the periods of 24 h and 1 week:

$$\Delta m = m(t) - m_o \qquad (5)$$

$$\Delta k = k(t) - k_o. \qquad (6)$$

Figure 10 provides a useful insight into the growth of stiffness independent of the measurement time and the effects of ambient temperature and relative humidity. As shown in figure 10, the stiffness growth is divided into slow, fast and steady-state stages. The wing stiffness grows at a slow rate in the initial stage, where Δm is from 0 to 0.5 mg. The wing stiffness increases by a maximum value of 0.12 mN mm^{-1} in the slow growth stage. The wing stiffness grows at a faster rate in the second stage, where Δm is between 0.5 and 1.2 mg. The maximum increase in wing stiffness is 0.75 mN mm^{-1} in the fast growth stage. The increased growth rate suggests that loss of water content might not be the only factor contributing
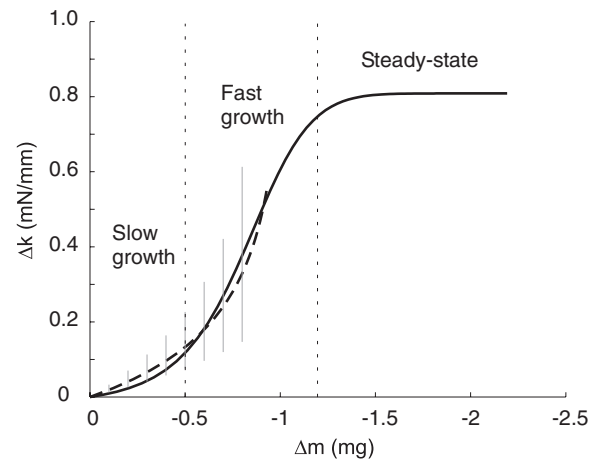

Figure 10. The change in stiffness as a function of the change in mass of the butterfly wings. The dark-dashed curve corresponds to Δm and Δk averaged for the five butterflies. The gray vertical lines show the range in Δk for the five butterflies. The dark-solid curve corresponds to Δm and Δk evaluated for the single butterfly measured over a 1 week period.

to the change in the stiffness of the wings in the second stage. Additional factors, such as changes in chemical composition of tissue, may be causing accelerated growth in the stiffness of the wings; however, this was not investigated in this work. Wing stiffness reaches a steady-state level in the final stage, where the decline in mass is above 1.2 mg. The maximum increase in wing stiffness at a steady-state level is 0.8 mN mm^{-1}.

The changes in mass and stiffness can have considerable consequences for computational analyses of insect flight. Incorporating erroneous data of mass and stiffness in structural models can significantly alter the results from the analyses. For example, modal analysis of a Painted Lady butterfly wing would yield incorrect values for the resonant frequencies, which are proportional to the square root of stiffness over mass [20, 21]. Assuming that the changes induced by desiccation are uniform throughout the wing, the percent change in the resonant frequencies can be determined using equation (7), where m_o and k_o are the initial mass and stiffness of the wing, respectively, and $m(t)$ and $k(t)$ are evaluated using equations (2) and (4). Figure 11 shows the percent change in the resonant frequencies due to desiccation over a 1 week period. The
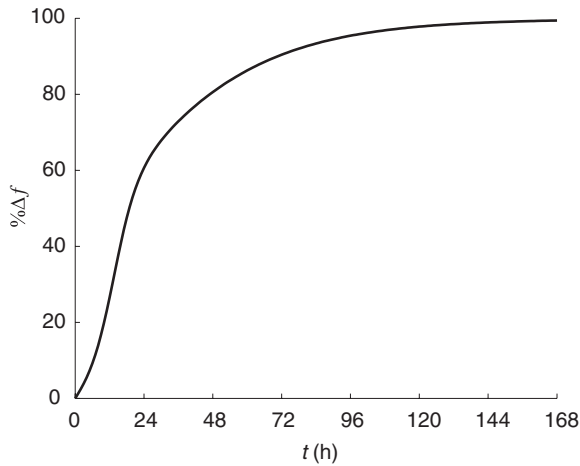
Figure 11. Percent change in the resonant frequencies of the butterfly wings due to desiccation over a 1 week period.

resonant frequencies would shift by 61% in the first 24 h, and by as much as 100% in 1 week:

$$\%\Delta f = \left(\sqrt{\frac{m_o \, k(t)}{k_o \, m(t)}} - 1 \right) \times 100. \qquad (7)$$

Computational and experimental analyses of insect flight provide the basis for the design of flapping MAVs. Inaccurate results from such studies can consequently lead to flawed designs of MAVs. The significance of desiccation must be recognized, and precautions should be taken to reduce its influence on the structural attributes of insect wings during experimental measurements. For example, using wings from freshly sacrificed insects, and limiting the duration of experiments can adequately minimize the effects of desiccation. The rate of desiccation is arguably affected by the level of ambient temperature and relative humidity. Further studies are necessary to investigate the effects of both temperature and humidity to establish a clear understanding that can be exploited for maintaining and controlling insect wing specimens.

Acknowledgments

References

[1] Ennos A R 1988 The importance of torsion in the design of insect wings *J. Exp. Biol.* **140** 137–60

[2] Combes S A and Daniel T L 2001 Shape, flapping and flexion: wing and fin design for forward flight *J. Exp. Biol.* **204** 2073–85

[3] Daniel T L and Combes S A 2002 Flexible wings and fins: bending by inertial or fluid-dynamic forces? *Integr. Comp. Biol.* **42** 1044–9

[4] Wootton R J 1992 Functional morphology of insect wings *Annu. Rev. Entomol.* **37** 113–40

[5] Dudley R 2000 *The Biomechanics of Insect Flight: Form, Function, Evolution* (Princeton, NJ: Princeton University Press)

[6] Chapman R F 1998 *The Insects: Structure and Function* (New York: Cambridge University Press)

[7] Hoffmann A A and Harshman L G 1999 Desiccation and starvation resistance in *Drosophila*: patterns of variation at the species, population and intrapopulation levels *Heredity* **83** 637–43

[8] Chown S L and Nicolson S W 2004 *Insect Physiological Ecology* (New York: Oxford University Press)

[9] Wootton R J, Evans K E, Herbert R and Smith C W 2000 The hind wing of the desert locust (*Schistocerca gregaria forskal*): I. Functional morphology and mode of operation *J. Exp. Biol.* **203** 2921–31

[10] Combes S A and Daniel T L 2003 Flexural stiffness in insect wings: I. Scaling and the influence of wing venation *J. Exp. Biol.* **206** 2979–87

[11] Steppan S J 2000 Flexural stiffness patterns of butterfly wings *J. Res. Lepidoptera* **35** 61–77

[12] Barbakadze N 2005 Micro/nanomechanical measurements on insect and plant cuticles *PhD Thesis* University of Stuttgart

[13] Smith C W, Herbert R, Wootton R J and Evans K E 2000 The hind wing of the desert locust (*Schistocerca gregaria forskal*): II. Mechanical properties and functioning of the membrane *J. Exp. Biol.* **203** 2933–43

[14] Richards F J 1959 A flexible growth function for empirical use *J. Exp. Bot.* **10** 290–301

[15] Birch C P D 1999 A new generalized logistic sigmoid growth equation compared with the Richards growth equation *Ann. Bot.* **83** 713–23

[16] Wagner T, Neinhuis C and Barthlott W 1996 Wettability and contaminability of insect wings as a function of their surface sculptures *Acta Zool.* **77** 213–25

[17] Zheng Y, Gao X and Jiang L 2007 Directional adhesion of superhydrophobic butterfly wings *Soft. Matter* **3** 178–82

[18] Goodwyn P P, Maezono Y, Hosoda N and Fujisaki K 2009 Waterproof and translucent wings at the same time: problems and solutions in butterflies *Naturwissenschaften* **96** 781–7

[19] Jones E F and Randall M S 2002 *Handbook of Mass Measurement* (Boca Raton, FL: CRC Press)

[20] Thompson W T and Dahleh M D 1998 *Theory of Vibration with Applications* 5th edn (Englewood Cliffs, NJ: Prentice-Hall)

[21] Palm W J 2007 *Mechanical Vibration* (New York: Wiley)